Journal of Ocean University of China (Oceanic and Coastal Sea Research)

ISSN 1672-5182, October 30, 2005, Vol.4, No.4, pp.315-328
http://www.ouc.edu.cn/xbywb/
E-mail: xbywb@mail.ouc.edu.cn

Simulating the Upper Ocean Circulation on the Belize Shelf: An Application of a Triply Nested-Grid Ocean Circulation Model

SHENG Jinyu[1),*], TANG Liqun[1,2)], and WANG Liang[1)]

1) *Department of Oceanography, Dalhousie University, Halifax, Nova Scotia, B3H 4J1, Canada*
2) *Department of Sedimentation Engineering, Institute of Water Resources and Hydropower Research, Beijing* 100044, *P.R. China*

(Received July 4, 2005; accepted October 7, 2005)

Abstract We present a three-level nested-grid ocean circulation modeling system for the Belize shelf of the western Caribbean Sea. The nested-grid system has three subcomponents: a coarse-resolution outer model of the western Caribbean Sea; an intermediate-resolution middle model of the southern Meso-American Barrier Reef System; and a fine-resolution inner model of the Belize shelf. The two-way nesting technique based on the semi-prognostic method is used to exchange information between the three subcomponents. We discuss two applications of the nested-grid system in this study. In the first application we simulate the seasonal mean circulation in the region, with the nested system forced by monthly mean surface fluxes and boundary forcing. The model results reproduce the general circulation features on the western Caribbean Sea and meso-scale circulation features on the Belize shelf. In the second application, we simulate the storm-induced circulation during Hurricane Mitch in 1998, with the nested-grid system forced by the combination of monthly mean forcing and idealized wind stress associated with the storm. The model results demonstrate that the storm-induced currents transport a large amount of estuarine waters from coastal regions of Honduras and Guatemala to offshore reef atolls.

Key Words two-way nesting; semi-prognostic method; numerical model; upper ocean process; storm-induced circulation; Hurricane Mitch

Number ISSN 1672-5182(2005)04-315-14

1 Introduction

The Belize Shelf (BS) is a narrow continental shelf in the northwest Caribbean Sea, bounded by Central America to the west, the Yucatan shelf to the north, the Yucatan Basin to the east, and the Gulf of Honduras to the south. The main topographic features of the BS (Fig.1) include the Belize Barrier Reef (BBR); three large off-shelf atolls known as Lighthouse Reef Atoll (LRA), Turneffe Islands Atoll (TIA) and Glovers Reef Atoll (GRA); and numerous patch reefs across the shelf (Macintyre and Aronson, 1997).

The coral reefs on the BS are important habitats, breeding and feeding grounds for a great diversity of marine invertebrates, fish, reptiles and mammals, with many sites in the region known to be used by reef fish spawning aggregations. Reef ecosystems are marine equivalents of terrestrial rainforests in terms of biodiversity (Hubbell, 1997), and they have significant economic value in terms of exploited resources, waste disposal, and protection of coastal property, and as a basis for tourism (Cesar, 2000; de Groot *et al.*, 2002). However, the reefs of the BS have been affected significantly by natural and anthropogenic factors, including hurricanes, disease outbreaks, coral bleaching and various disturbances and stresses resulting from human activities in the region over the last 30 yr (Gibson *et al.*, 1998; Williams and Bunkley-Williams, 2000). Thus, there is an increasing demand for a better understanding of the physical, ecological and biological processes that connect and sustain the marine ecosystems of the BS and the broader Caribbean Sea.

The circulation on the BS is part of the large-scale circulation on the Caribbean Sea. The latter has been studied in the last hundred years (Wust, 1964; Gordon, 1967; Roemmich, 1981; Gallegos, 1996; Kinder *et al.*, 1985; Maul, 1993; Murphy *et al.*, 1999; Johns *et al.*, 2002; Sheng and Tang, 2003). Readers are referred to Mooers and Maul (1998) for a comprehensive overview of oceanography of the region. The upper ocean circulation on the BS is dominated by a persistent throughflow known as the Caribbean Current, which enters the northwestern Caribbean Sea along the outer flank of Nicaragua Rise, and then flows westward about 200 to 300 km off the northern coast of Honduras. The Caribbean Current veers anticyclonically to flow northward along the eastern coast of Belize and Mexico after passing the Gulf of Honduras (GOH). The physical processes on the BS are also sig-

* Corresponding author. Tel: (902) 494-2718
E-mail: Jinyu.Sheng@Dal.Ca

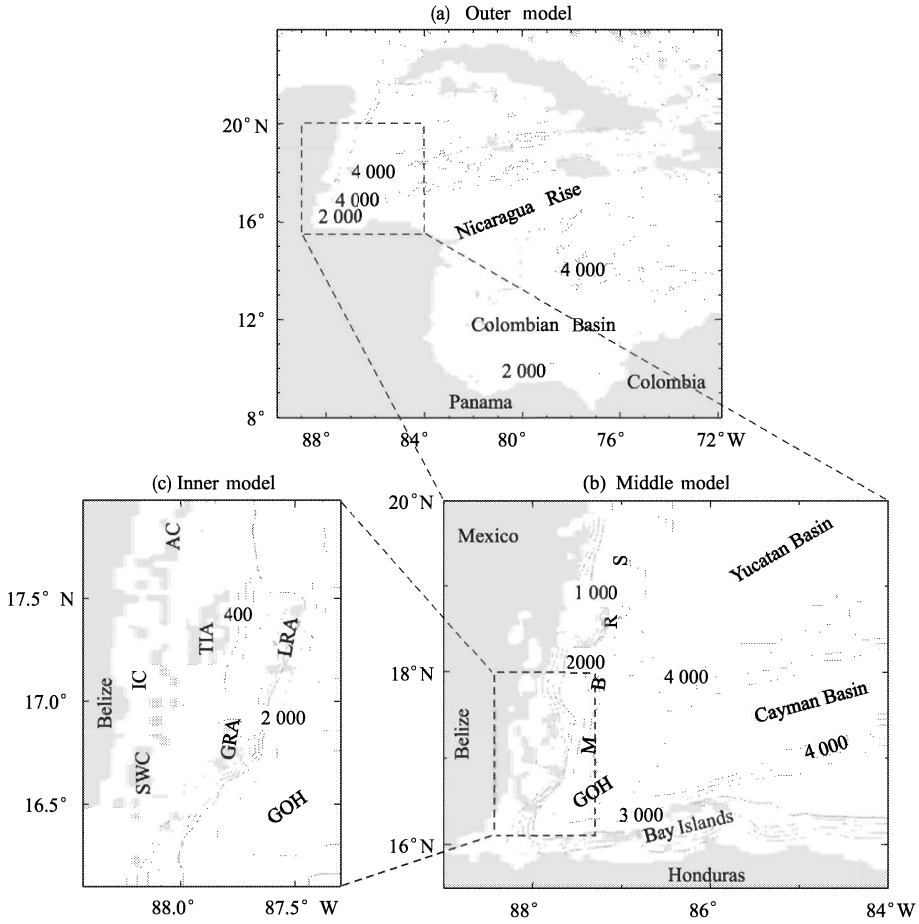

Fig.1 Selected bathymetric features for the triply nested-grid modeling system, which consists of (a) an outer model covering the western Caribbean Sea (WCS); (b) a middle model covering the southern Meso-American Barrier Reef System (MBRS); and (c) an inner moldel covering the Belizean shelf (BS). Abbreviations are used for Lighthouse Reef Atoll (LRA), Turneffe Islands Atoll (TIA), Glovers Reef Atoll (GRA), South Water Cay (SWC), Inner Channel (IC), and Ambergris Cay (AC). Contours are labeled in units of meters.

nificantly affected by the freshwater runoff from rivers in the region. For instance, after Hurricane Mitch in 1998, the turbid waters from the rivers along the coastline of Honduras and Guatemala reached the Bay Islands in less than one day and reached Belize's offshore atolls within five days. During the same period, the estuarine plumes from Honduras extended more than 300 km in three days towards Chinchorro Bank atoll. A three-dimensional ocean circulation model is required to resolve the general circulation and water mass distributions on the BS at various temporal and spatial scales.

Various numerical ocean circulation models have been used to study the general circulation and water mass distribution in the Caribbean Sea. Kinder *et al*. (1985) used a reduced-gravity ocean model to study the formation and propagation of mesoscale eddies in the upper ocean of the southeastern Caribbean Sea. Hurlburt and Townsend (1994) applied the Naval Research Laboratory layered ocean model (NLOM) to the Caribbean Sea and the Gulf of Mexico. Mooers and Maul (1998) applied the terrain-following Princeton Ocean Model to the Intra-Americas Sea (IAS). Murphy *et al*. (1999) applied the NLOM to the IAS and examined the connectivity of the CS eddies with the Atlantic Ocean and the Gulf of Mexico. Johns *et al*. (2002) applied the same NLOM to the Atlantic Ocean from 20°S to 65°N. Sheng and Tang (2003) used a z-level ocean circulation model to examine the mean circulation and associated seasonal variability in the western Caribbean Sea. Tang *et al*. (2005)① recently used a three-dimensional ocean circulation model to examine the hydrodynamic connectivity among reefs in the southern Meso-American Barrier Reef System (MBRS). The main purpose of this study is to use a three-level nested-grid ocean circulation modeling system to study the monthly mean circulation and storm-induced currents in the surface waters of the BS.

The organization of this paper is as follows. We describe the nested-grid modeling system and model forcing in Section 2, and discuss the monthly mean

① Tang, L., J. Sheng, B. Hatcher, and P. Sale, 2005. Numerical study of circulation, dispersion and hydrodynamic connectivity of surface waters on the Belize shelf. *J. Geophs. Res.*, (in press).

circulations in the upper ocean in Section 3. Section 4 presents the storm-induced circulation during Hurricane Mitch. Section 5 is a summary and conclusion.

2 The Nested-Grid Ocean Circulation Modeling System and Model Forcing

The nested-grid ocean circulation modeling system used in this study is based on the three-dimensional, primitive-equation, ocean circulation model known as CANDIE (Canadian version of DieCAST (Sheng *et al.*, 1998)). CANDIE has been successfully applied to various modeling problems on the continental shelf. The most recent applications of the model include the numerical studies of the storm-induced circulation on the Scotian Shelf (Sheng *et al.*, 2005 a)①, seasonal circulation in the western Caribbean Sea (Sheng and Tang, 2003, 2004; Tang *et al.*, 2005②), and nonlinear tidal circulation in coastal waters (Sheng and Wang, 2004).

The nested-grid modeling system has a three-level nesting structure, with an outer model covering the western Caribbean Sea (WCS, 8°–25°N, 72°–90°W), a middle model covering the southern part of the Meso-American Barrier Reef System (MBRS, 15.5°–20°N, 84°–89°W), and an inner model covering the BS (16.1°–18°N, 87.38°–88.5°W), except where indicated otherwise. Horizontal resolutions are approximately 19 km for the outer model, 6 km for the middle model, and 2 km for the inner model, respectively. All the three subcomponents have the same 31 unevenly spaced z-levels, with the centers of each level located respectively at 5, 16, 29, 44, 61, 80, 102, 128, 157, 191, 229, 273, 324, 383, 450, 527, 615, 717, 833, 967, 1 121, 1 297, 1 500, 1 733, 2 000, 2 307, 2 659, 3 063, 3 528, 4 061, and 4 673 m. The nested system uses the bathymetry database of 2-minute resolution (DBDB2) developed by the Ocean Dynamics and Prediction Branch, the Naval Research Laboratory of the United States (Dong-Shan Ko, personal communication, 2003; http://www7320.nrlssc.navy.mil/DBDB2_WWW).

The nested-grid system uses the newly developed two-way nesting technique based on the smoothed semi-prognostic (SSP) method (Sheng *et al.*, 2005 b)③. The SSP nesting technique is equivalent to adding an interaction term to the model momentum equation in each sub-component of the nested system. Readers are referred to the Appendix for more discussion on the SSP nesting technique.

The nested system uses the vertical mixing scheme of Large *et al.* (1994) for vertical eddy viscosity and diffusivity coefficients (K_m and K_h), and the horizontal mixing scheme of Smagorinsky (1963) for the horizontal eddy viscosity coefficient A_m. The horizontal turbulent Prandtl Number A_h/A_m is set to 0.1, where A_m is the horizontal eddy diffusivity coefficient. Since the Smagorinsky scheme is resolution dependent, it has the desirable effect of having different levels of horizontal mixing in the different subcomponents of the nested system. The nested system also uses the fourth-order numerics suggested by Dietrich (1997) and flux limiter suggested by Thuburn (1996) to discretize the nonlinear advection terms.

The model boundary conditions used in this study are as follows. At lateral solid boundaries, the normal flow, tangential stress of the currents and horizontal fluxes of temperature and salinity are set to zero (*i.e.*, free-slip conditions). Along open boundaries of each subcomponent, the normal flow, temperature and salinity fields are calculated using adaptive open boundary conditions (Marchesiello *et al.*, 2001). The model first uses an explicit Orlanski radiation condition (Orlanski, 1976) to determine whether the open boundary is passive (outward propagation) or active (inward propagation). If the open boundary is passive, the model prognostic variables are radiated outward to allow any perturbation generated inside the model domain to propagate outward as freely as possible. If the open boundary is active, the outer model prognostic variables at the open boundary are restored to the monthly mean climatology with a restoring time scale of 15 d, and the middle and inner model prognostic variables at the open boundary are restored to the outer and middle model results respectively, with a restoring time scale of 5 h. In addition, the depth-mean normal flows across the outer model open boundaries are set to the monthly mean results produced by a (1/3)° Atlantic model (Carsten, 2003)④ based on FLAME (Family of Linked Atlantic Model Experiments; Dengg *et al.*, 1999).

The nested-grid modeling system is initialized with January mean climatology of temperature and salinity (TS), and forced by the climatological monthly-mean surface wind stress and heat flux constructed by da Silva *et al.* (1994). The net heat flux through the sea surface Q_{net} is expressed by Barnier *et al.* (1995) as:

$$Q_{net} = Q_{net}^{clim} + \gamma(SST^{clim} - SST^{model}), \qquad (1)$$

where Q_{net}^{clim} is the monthly mean net heat flux taken from da Silva *et al.* (1994), SST^{clim} is the monthly mean sea surface temperature, and γ is the coupling

① Sheng, J., X. Zhai, and R. J. Greatbatch, 2005 a. Numerical study of the storm-induced circulation on the Scotian Shelf during Hurricane Juan using a nested-grid ocean model. *Prog. in Oceanogr.*, (in press).

② Tang, L., J. Sheng, B. Hatcher, and P. Sale, 2005. Numerical study of circulation, dispersion and hydrodynamic connectivity of surface waters on the Belize shelf. *J. Geophs. Res.*, (in press).

③ Sheng, J., R. J. Greatbatch, X. Zhai, and L. Tang, 2005 b. A new two-way nesting technique based on the smoothed semi-prognostic method. *Ocean Dyn.*, (in press).

④ Carsten Eden, 2003. Personal communication.

coefficient defined as $\Delta z_1 \rho_0 c_p / \tau_Q$, where Δz_1 is the thickness of the top z-level, c_p is the specific heat, and τ_Q is the restoring time scale which is set to 15 d. The implied value of γ is about 35 W m^{-2} K^{-1}, which is comparable to values calculated from the observations (*e. g.* Haney, 1971). We also restore the model sea surface salinity to the monthly mean climatology on a time scale of 15 d.

3 Monthly Mean Circulation and Temperature Distributions

The nested-grid modeling system is first used to simulate the general circulation and the associated seasonal variability in the western Caribbean Sea and meso-scale circulation features on the BS. In this application, the nested-grid system is initialized with January mean temperature/salinity (TS) climatology and integrated for five years (control run). The model results of the last four years are used to calculate monthly mean circulation and TS fields.

Figs. 2 to 5 show the monthly mean near-surface (5 m) temperature in four different months of February, May, August and November, respectively. The February mean near-surface temperature produced by the course-resolution outer model (Fig.2 a) has small-horizontal variations and is about 26.5 ℃ on average in the WCS, except for the eastern and northern Yucatan Basin and eastern Cayman Basin where the near-surface temperature is about 25 ℃. There is a cold water pool associated with coastal upwelling over the coastal region off northeast Colombia in February, with some cold waters advected northwestward by near-surface currents. The February mean near-surface temperature produced by the finer-resolution middle model (Fig.2 b) has similar horizontal distributions as the outer model results in the southern MBRS, except for more small-scale features produced by the middle model in the coastal regions. The February mean near-surface temperature in the BS produced by the finest-resolution inner model (Fig.2 c) is characterized by about 26 ℃ over the central and southern BS and slightly colder, or about 25.5 ℃, over the three offshore atolls of LHA, TIA and GRA.

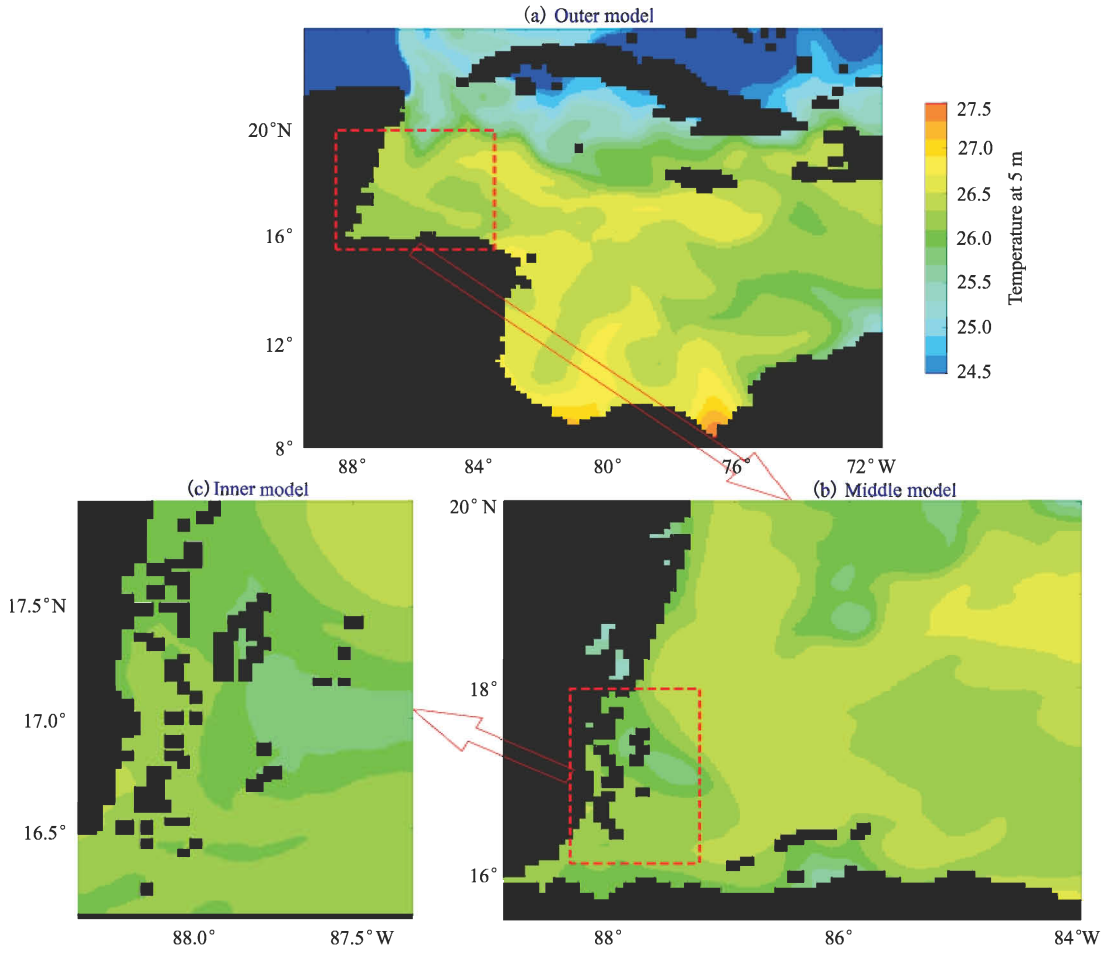

Fig.2 February mean near-surface (5 m) temperature calculated from 4-a model results produced by (a) the outer model, (b) middle model, and (c) inner model of the nested-grid system.

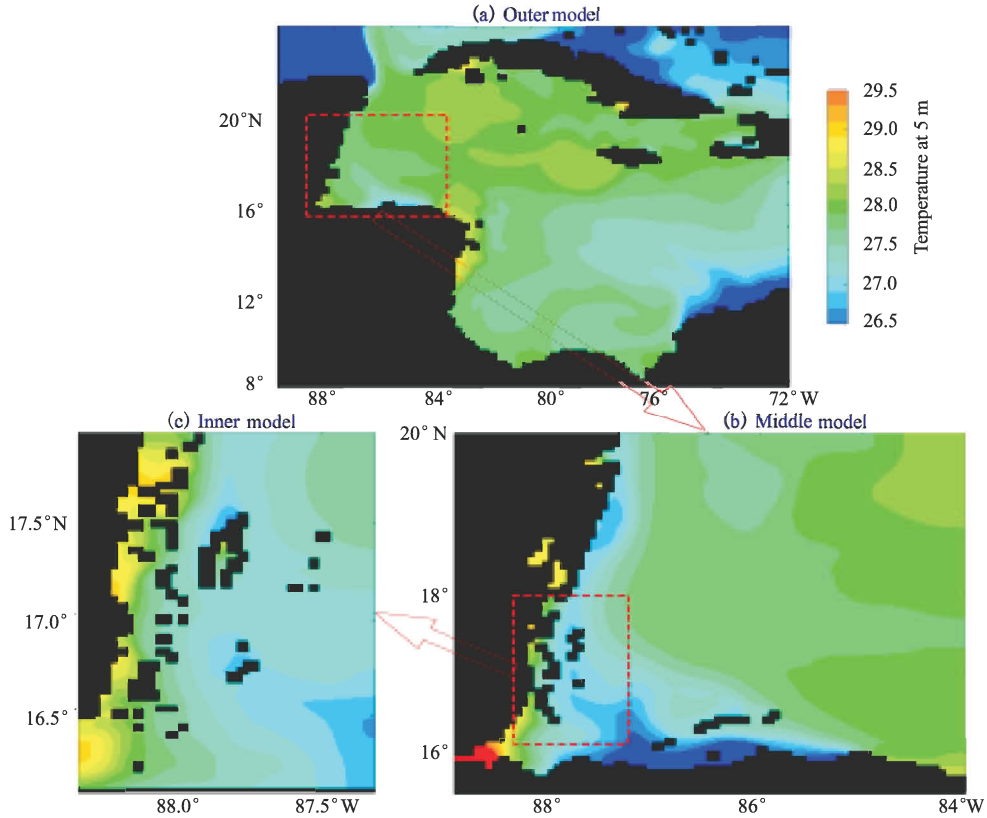

Fig.3 May mean near-surface (5 m) temperature calculated from 4-a model results produced by (a) the outer model, (b) middle model, and (c) inner model of the nested-grid system.

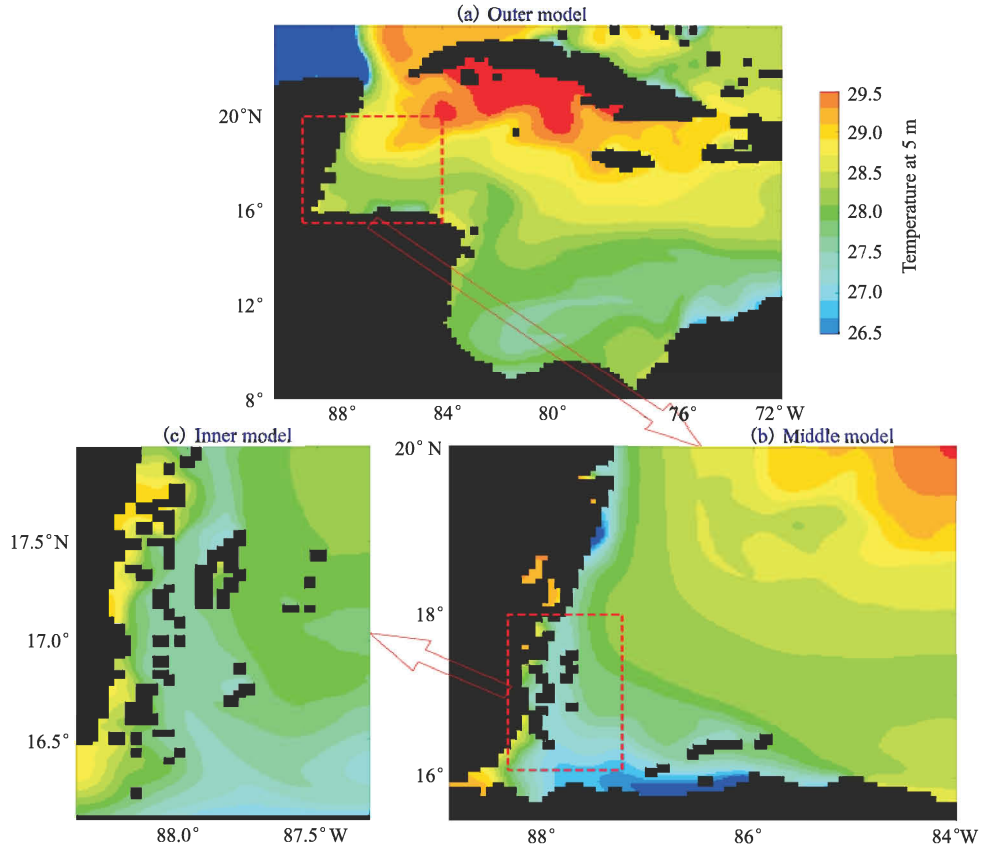

Fig.4 August mean near-surface (5 m) temperature calculated from 4-a model results produced by (a) the outer model, (b) middle model, and (c) inner model of the nested-grid system.

The May mean near-surface temperature produced by the outer model (Fig.3 a) also has small horizontal variations in the WCS and is about 27.5 ℃ on average, except for slightly lower temperature over the coastal regions off northeastern Colombia and northern Honduras (Fig.3 a). Some cold surface waters near the coast of northern Honduras are transported northwestward to the outer shelf of the BS (Fig.3 b). Over the inner BS, the near-surface temperature is about 29 ℃ (Fig.3 c), which is slightly warmer than that over theouter BS and offshore atolls.

The monthly mean near-surface waters in August are characterized by a relatively warmer temperature of about 29 ℃ over the eastern parts of the Yucatan and Cayman Basins and a relatively colder temperature of about 27.5 ℃ over the western Colombian Basin (Fig.4 a). There are also two well-defined coastal upwelling areas in August, with one off northeastern Colombia and the other off northern Honduras (Fig.4 b). Relatively cold near-surface waters of about 27 ℃ are advected northwestward to affect the offshore areas of BS. The temperatures of the coastal waters of the BS are about 29 ℃ in August (Fig.4 c).

The near-surface temperature in November is about 27.5 ℃ over the northeastern Colombian Basin and southeastern Cayman Basin (Fig.5 a). The near-surface temperature in the southern MBRS produced by the middle model is uniform and slightly colder, *i.e.*, about 26 ℃ (Fig.5 b). On the BS, the near surface temperature is relatively cold over the coastal region and southern BS, and relatively warm over the offshore atolls (Fig.5 c).

We next examine the monthly mean currents calculated from the nested-grid model results of the last 4 yr of simulations. The monthly mean, near-surface (5 m) currents in the WCS produced by the outer model in the four months of February, May, August and November have similar overall circulation features (see outer model results in Figs.5 to 9), and are characterized by a persistent throughflow known as the Caribbean Current, which is relatively broad and roughly westward in the central and eastern Colombian Basin. The Caribbean Current bifurcates before reaching the Nicaragua Rise, with a weak branch veering southwestward to form the cyclonic, highly variable Panama-Colombia Gyre in the southwestern Caribbean Sea. The main branch of the Caribbean Current turns northwestward and flows along the outer flank of Nicaragua Rise to form a narrow offshore flow running westward and then northward to the Gulf of Mexico. The main features of the general circulation produced by the outer model are in good agreement with the current knowledge of the general circulation in the WCS (Maul, 1993; Mooers and Maul, 1998; Johns *et al.*, 2002; Ezer *et al.*, 2003).

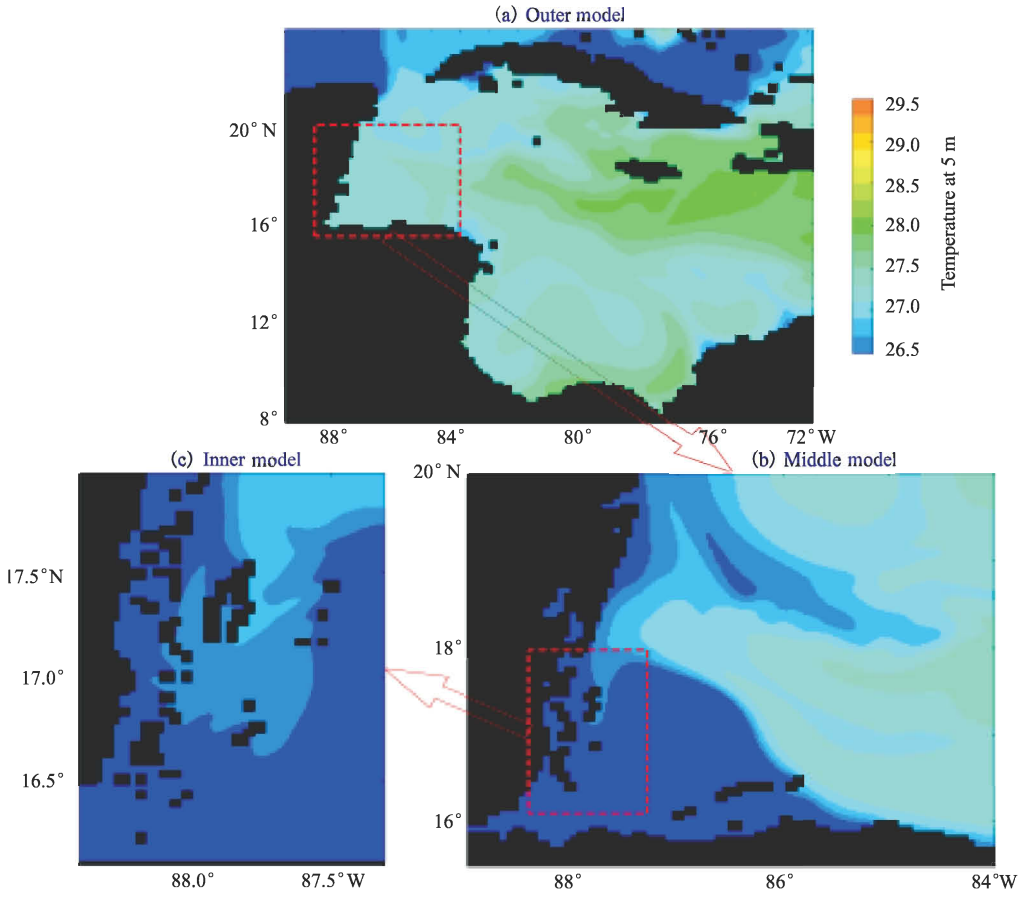

Fig.5 November mean near-surface (5 m) temperature calculated from 4-a model results produced by (a) the outer model, (b) middle model, and (c) inner model of the nested-grid system.

The near-surface currents produced by the coarse-resolution outer model have significant month-to-month variability (Tang *et al.*, 2005)①. The Caribbean Current is relatively stronger in August and weaker in other three months (February, May and November). The Panama-Colombia Gyre is made up of two cyclones in August and November, but only a single cyclone in February and May. The highly variable behaviors of the Panama-Colombia Gyre produced by the nested system are consistent with previous findings based on satellite altimetry data (Nystuen and Andrade, 1993; Andrade and Barton, 2000) and near-surface drifter data (Fratantoni, 2001).

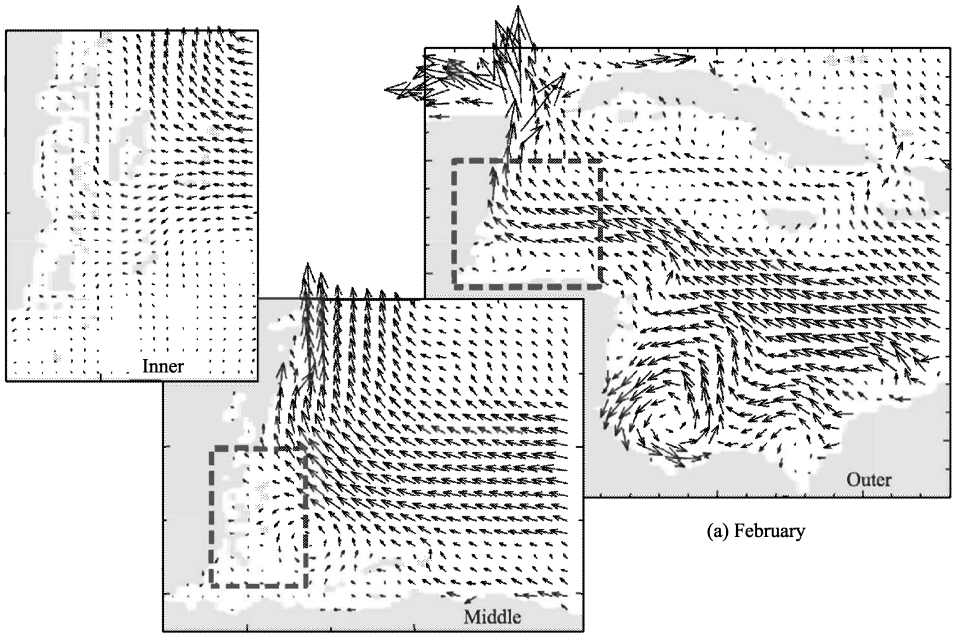

Fig.6 February mean near-surface (5 m) currents calculated from 4-a model results produced by the nested-grid system. Velocity vectors are plotted at every third model grid point.

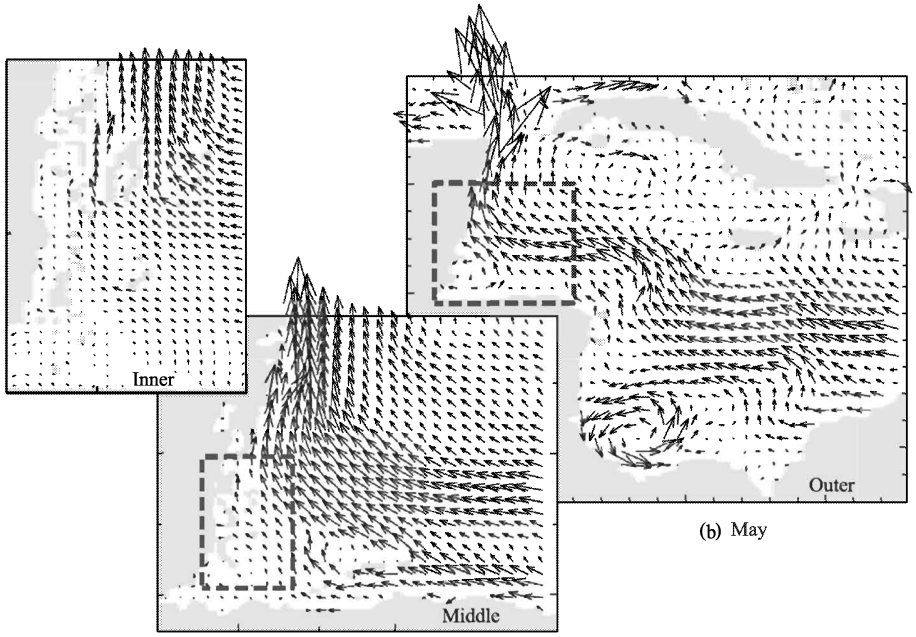

Fig.7 May mean near-surface (5 m) currents calculated from 4-a model results produced by the nested-grid system. Velocity vectors are plotted at every third model grid point.

The monthly mean near-surface currents produced by the intermediate-resolution middle model in the selected four months (see middle model results in Figs.5 to 9) are dominated by the Caribbean Current that runs first westward in the deep water off the continen-

① Tang, L., J. Sheng, B. Hatcher, and P. Sale, 2005. Numerical study of circulation, dispersion and hydrodynamic connectivity of surface waters on the Belize shelf. *J. Geophs. Res.*, (in press).

tal shelf of Honduras, and then turns northward as it approaches the Gulf of Honduras (GOH) to form an intense coastal jet running northward along the east coast of Belize and Mexico. The near-surface currents produced by the middle model also have significant month-to-month variability. The Caribbean Current in the region is relatively stronger in May and August and weaker in February and November. In addition, there is a small-scale cyclonic recirculation associated with the Honduras Convergence in February and November. This recirculation does not appear, however, in May and August.

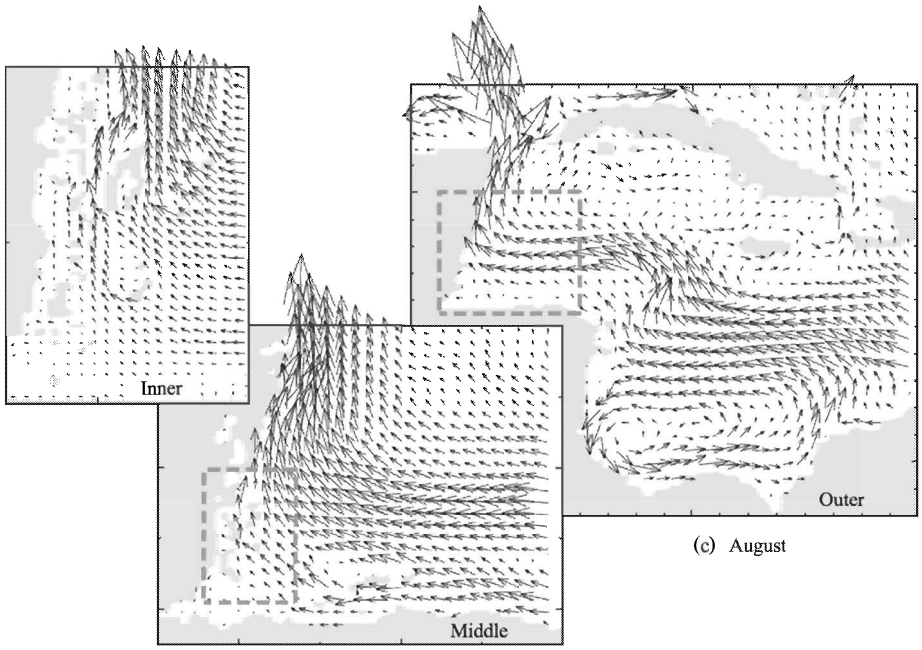

Fig.8 August mean near-surface (5 m) currents calculated from 4-a model results produced by the nested-grid system. Velocity vectors are plotted at every third model grid point.

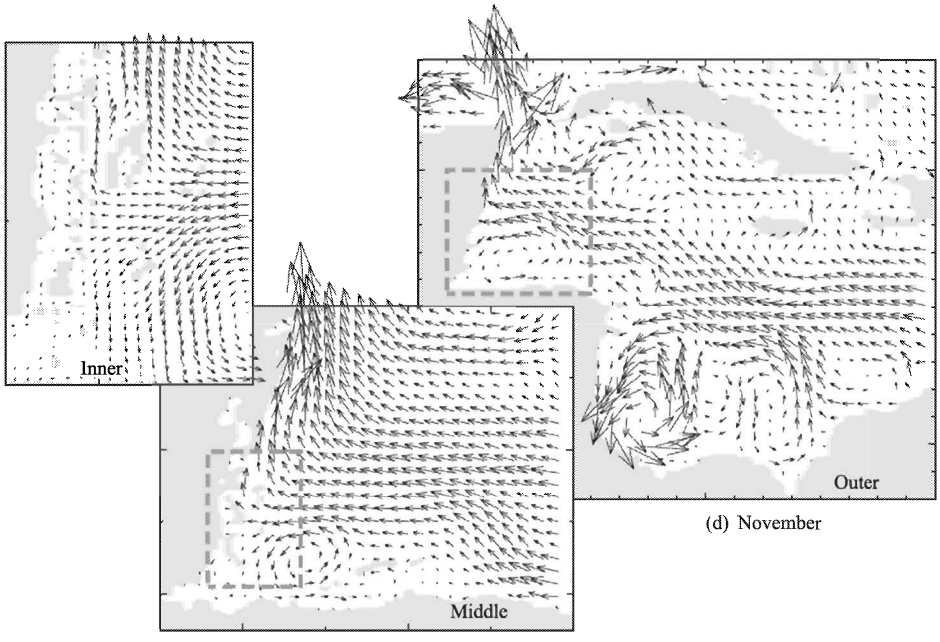

Fig.9 November mean near-surface (5 m) currents calculated from 4-a model results produced by the nested-grid system. Velocity vectors are plotted at every third model grid point.

The fine-resolution inner model produces more mesoscale circulation features than the outer and middle models over the BS (Figs.5－9). In the area seaward (east) of Lighthouse Reef Atoll (LRA) and Turneffe Islands Atoll (TIA), the monthly mean near-surface currents produced by the inner model are strong and approximately northwestward, a direct influence of the Caribbean Current in these areas. The

near-surface currents separate into two branches before reaching the southeastern margin of TIA, with the main branch veering anti-cyclonically to flow northward to the deep waters of the Belize barrier reef (BBR), and a weak branch flowing around the south tip of TIA before turning northward through a narrow passage between TIA and the BBR. The monthly mean currents are spatially variable within the Inner Channel (IC) and in reef areas off Glovers Reef Atoll (GRA) and South Water Cay (SWC). The monthly mean near-surface currents in the eastern margin of LRA and TIA are relatively weaker in February and November and stronger in May and August. Over the southern BS, the near-surface currents are relatively weaker in February and May and stronger in August and November. The monthly mean near-surface circulation in February and November produced by the inner model separates into three branches before reaching the southeast margin of TIA: one branch turning northward, a second branch turning southward to form a cyclonic recirculation in the GOH, and a third branch running westward through the passage between TIA and GRA before spreading onto the reef areas within the IC. In contrast, during May and August the near-surface currents in the southern BS are all approximately northwestward.

It should be noted that the three subcomponents (*i.e.*, the outer, middle and inner models) of the nested-grid modeling system generate very similar large-scale features of monthly mean near-surface circulation and TS fields over the BS, which demonstrates the advantage of the newly-developed two-way nesting tec-

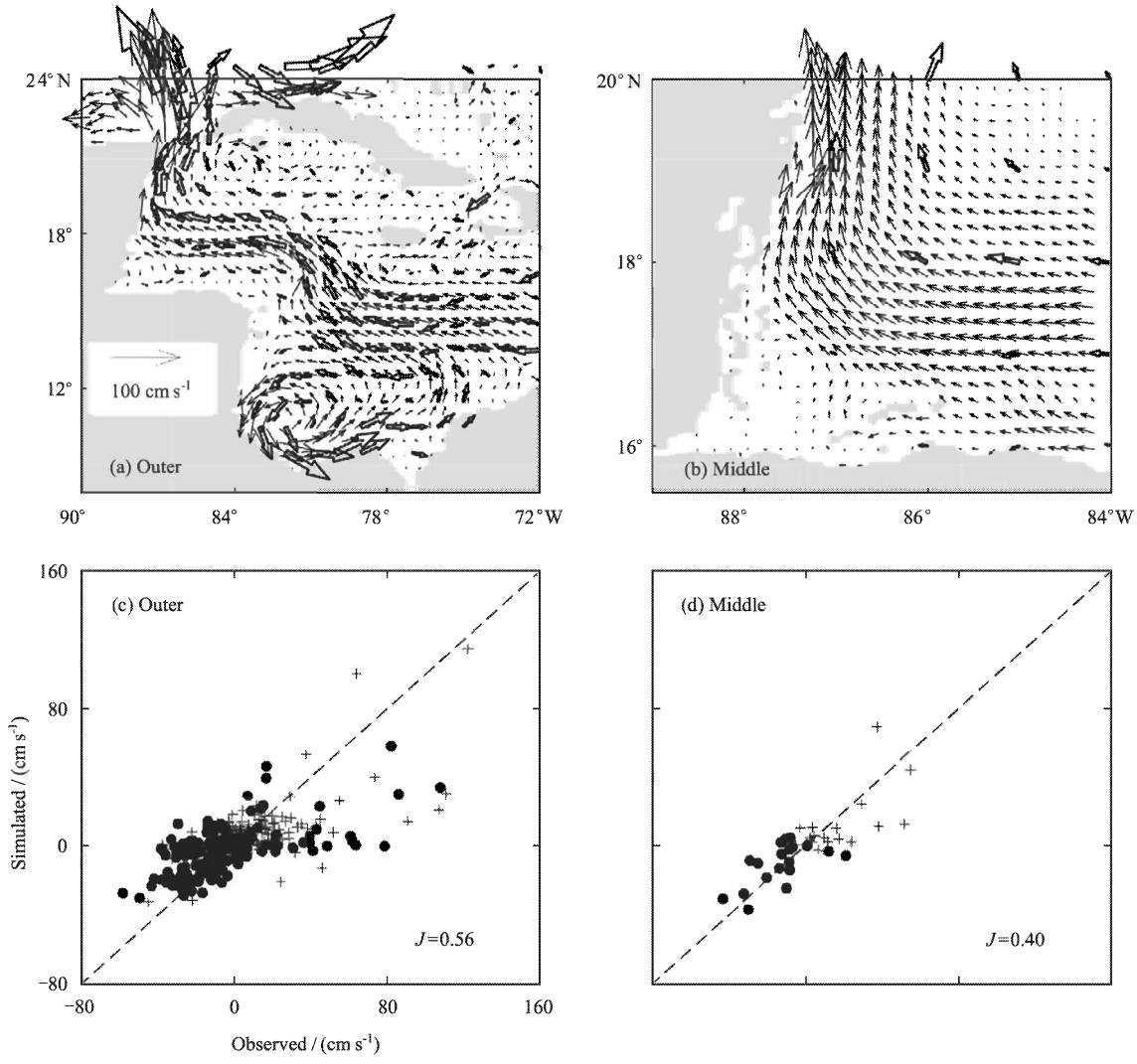

Fig.10 Comparison of modeled (solid arrows) and observed (open arrows) currents (a) in the western Caribbean Sea (WCS) and (b) in the southern Meso-American Barrier Reef System (MBRS). The modeled currents in the WCS and southern MBRS are the annual mean currents at 16 m produced by the nested-grid outer and middle models respectively. The observed currents are the grid time-mean currents during the 1990s inferred from trajectories of 15 m-drogued satellite-tracked drifters by *Fratantoni* (2001) on a 1° grid. Scatter plots of observed and model-calculated time-mean currents (c) in the WCS and (d) in the southern MBRS (adopted from Tang *et al.* (2005)).

hnique. As stated in Sheng *et al.*, (2005 b)①, the new twoway nesting technique based on the semi-prognostic method effectively prevents unrealistic drift of the three subcomponents of the nested system. An examination of the instantaneous model results (not shown) also indicates that the fine-resolution inner model produces more small-scale features of instantaneous currents than the intermediate-resolution middle model and much more than the coarse-resolution outer model (see also Section 4).

Tang *et al.* (2005)② assessed the performance of the nested-grid system by comparing the annual mean currents at 16 m depth produced by the outer and middle models with the time-mean currents inferred from trajectories of the satellite-tracked 15-m drogue drifters made during the 1990s (Fratantoni, 2001). The results of the nested-grid outer model reproduce reasonably well the large-scale features of the observed currents in the WCS, including the persistent Caribbean Current throughflow and the intense Panama-Colombia Gyre (Fig.10 a). The middle model results also reproduce reasonably well the observed currents in the southern MBRS.

To quantify the model performance, Tang *et al.* (2005)③ calculated the misfit between the empirical observations and the model-computed currents based on J, defined as:

$$J = \frac{\sum_{k}^{N} \left[(u_k^o - u_k^s)^2 + (v_k^o - v_k^s)^2 \right]}{\sum_{k}^{N} \left[(u_k^o)^2 + (v_k^o)^2 \right]}, \qquad (2)$$

where (u_k^o, v_k^o) are the horizontal components of the observed currents at the *kth* location estimated by Fratantoni (2001), (u_k^s, v_k^s) are the horizontal components of the simulated currents produced by the outer or middle models at the same *kth* location as the observations respectively, and N is the total number of locations where observations were made. The smaller value of J, the better the model results fit the observations. The J value is about 0.54 for the outer model results in the WCS (see Fig.10 c), and about 0.40 for those in the southern MBRS (not shown). The J value for the middle model results in the southern MBRS is also about 0.40 (Fig.10 d). Therefore, both the nested-grid middle and outer models perform reasonably well in simulating Fratantoni's observed currents in the study region. Comparison of the inner model results with the time-mean observed currents in the BS was not attempted mainly because Fratantoni's data do not resolve the fine-scale circulation features in the BS.

4 The Storm-Induced Circulation During Hurricane Mitch

The second application of the nested-grid modeling system is the numerical simulation of storm-induced circulation over the southern MBRS during Hurricane Mitch in later October and early November 1998. Hurricane Mitch was one of the most deadly and catastrophic hurricanes of our time that struck the Central American countries of Nicaragua, Honduras, El Salvador and Guatemala. Eleven thousand people were confirmed dead and more than ten thousand people were reported missing. Estimated property damage exceeded 5 billion in US dollars.

Hurricane Mitch originated as a tropical depression over the southwestern Caribbean Sea to the north of Colombia on October 22, 1998 (http://www.nhr.noaa.gov). The storm slowly moved westward and became a tropical storm later that day (Fig.11). It turned northward and became a hurricane by October 24. Mitch turned westward again and intensified rapidly to become a Category 5 hurricane on the Saffir-Simpson Scale. By 2100 UTC (Universal Time Coordinated) on October 26, the storm had deepened to a central pressure of 905 hPa with sustained winds of 290 km h^{-1} and gusts over 320 km h^{-1}. Mitch remained at Category 5 status for a continuous period of 33 h, with sustained winds of 295 km h^{-1} for 15 h. Mitch passed over the Swan Islands on October 27, and weakened slightly as it approached Honduras. As Mitch neared the coast, its forward motion stopped and meandered off the coast of Honduras until the 29th. Hurricane Mitch ravaged the offshore islands of Honduras with high winds, seas, and storm surge, and eventually weakened into a tropical depression by the time it entered Guatemala on October 31.

In comparison with the first application of the nested system presented in Section 3, there are four major differences in the model setup and forcing in order to better simulate the near-surface circulation and TS distributions induced by Hurricane Mitch over the southern MBRS. First, the inner model domain covers the coastal and shelf waters around Bay Islands off Honduras (15.6°–17°N, 85°–88°W). Second, the three components of the nested-grid modeling system have 28 z-levels with the centers of the levels located respectively at 1, 3, 5, 7, 9, 11, 13, 15, 17, 19, 25, 40, 75, 140, 230, 340, 450, 575, 725, 900, 1 250, 1 750, 2 250, 2 750, 3 250, 3 750, 4 250, 4 750 m. Third, the model forcing is forced by the monthly mean forcing as in the control run during the first 290 d and then by the combination of the monthly mean forcing described in Section 3 and the idealized wind

① Sheng, J., R. J. Greatbatch, X. Zhai, and L. Tang, 2005 b. A new two-way nesting technique based on the smoothed semi-prognostic method. *Ocean Dyn.*, (in press).

② Tang, L., J. Sheng, B. Hatcher, and P. Sale, 2005. Numerical study of circulation, dispersion and hydrodynamic connectivity of surface waters on the Belize shelf. *J. Geophs. Res.*, (in press).

③ Same as ②.

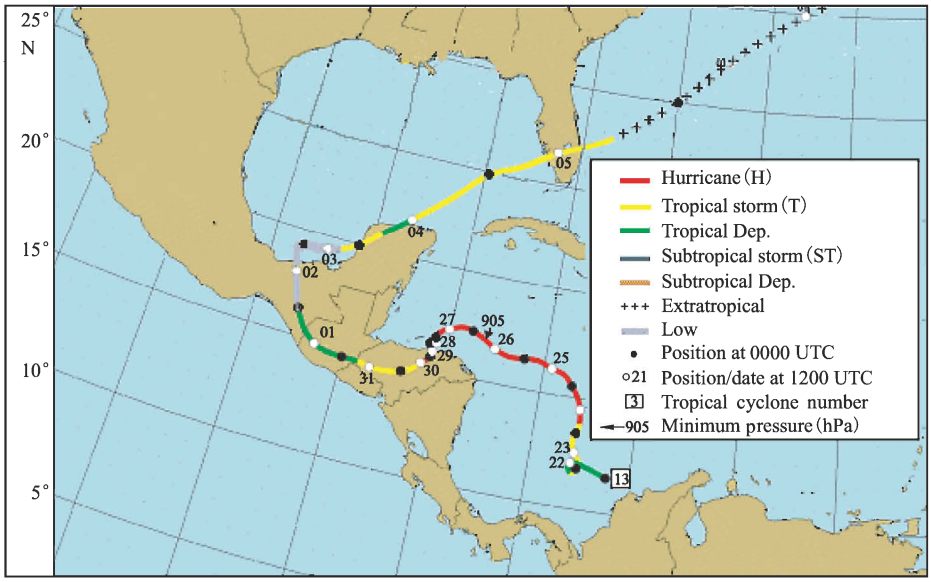

Fig.11 Storm track of Hurricane Mitch in late October and early November 1998 compiled by GeoResources (www.geosources.co.uk).

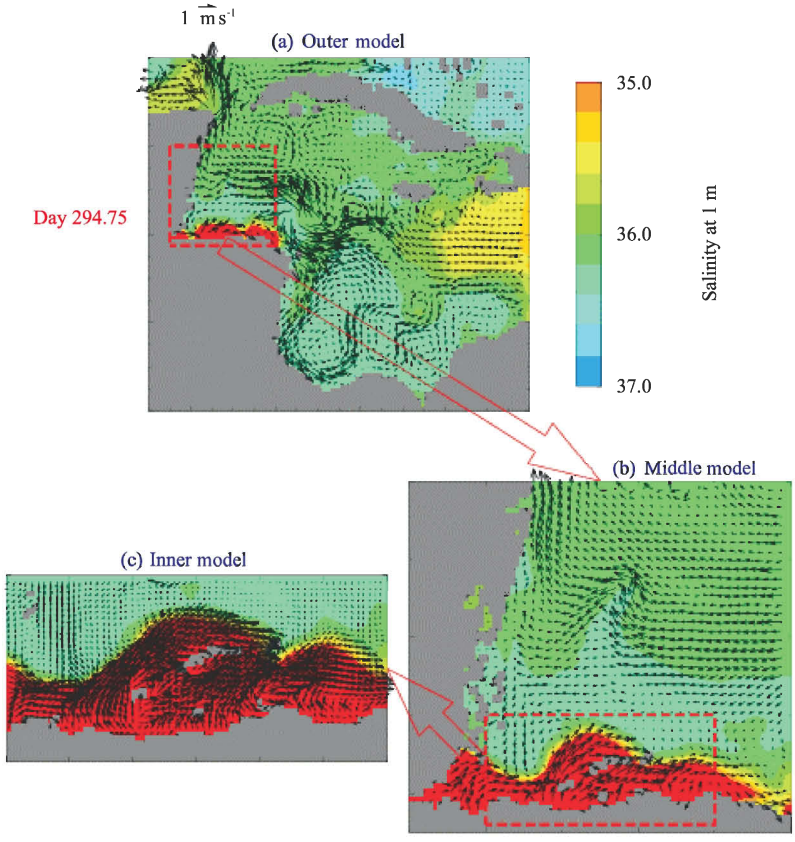

Fig.12 Instantaneous near-surface (5 m) currents and salinity at yearday 294.75 during Hurricane Mitch in 1998. Velocity vectors are plotted at every second model grid point.

stress associated with Hurricane Mitch after 290 d. The latter is based on the parameterization suggested by Chang and Anthes (1978) and the observed storm track shown in Fig.11. Fourth, the near-surface salinity along the central coast of Honduras is set to 10×10^{-12} to represent the influence of freshwater runoff during Hurricane Mitch in late October 1998.

Fig.12 shows the instantaneous near-surface currents and salinity produced by the nested-grid modeling 16.9° N and 83.1° W. The model results show strong system at yearday 294.75 (October 26), 1998. At this time the center of Hurricane Mitch was located

at divergent currents under the storm and intense inertial currents behind the storm. A large amount of freshwater is advected offshore to affect the near-surface salinity and circulation around Bay Islands. At yearday 302.75 (November 3), the center of the storm was located in the Gulf of Mexico (Fig.11). The near-surface currents are intense in the southern MBRS, with several recirculation features in the southern MBRS around Bay Island. Associated with the intense near-surface currents, coastal plumes are entrained into the offshore regions off Bay Island, the overall features agreeing reasonably well with the remote sensing ocean color data.

Finally, a comparison of Figs.12 and 13 with Fig.9 demonstrates that there are significantly large differences in the near-surface circulations over the southern MBRS produced by the nested-grid system with and without storm forcing, indicating that Hurricane Mitch

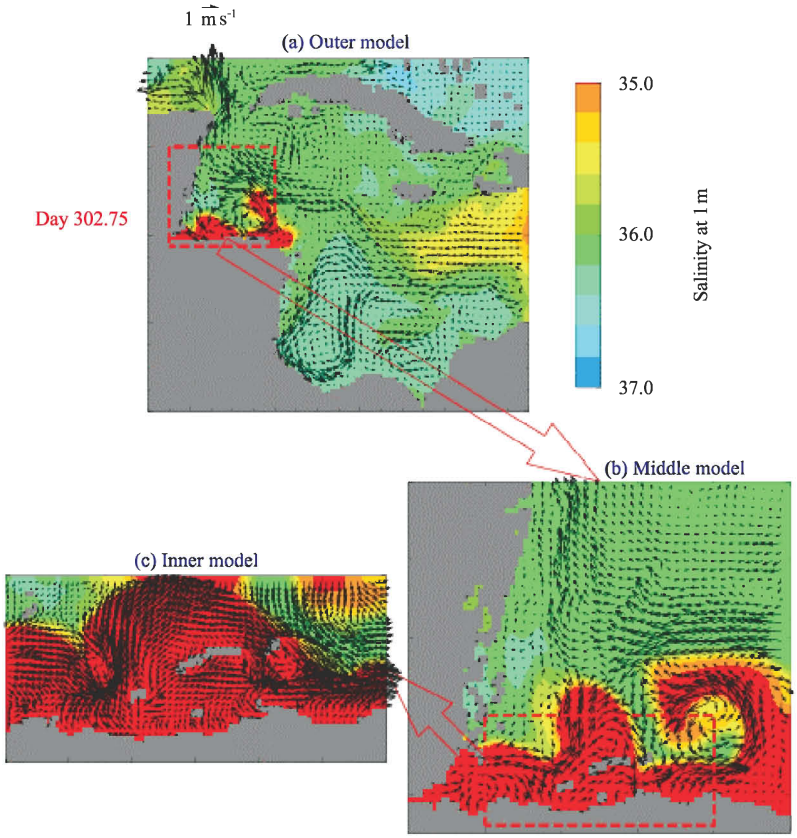

Fig.13 Instantaneous near-surface (5 m) currents and salinity at yearday 302.75 during Hurricane Mitch in 1998. Velocity vectors are plotted at every second model grid point.

introduced significant changes to the circulation and TS distributions in the upper ocean of the southern MBRS.

5 Summary and Conclusion

A three-level nested-grid ocean modeling system was used to simulate the hydrodynamic circulation and water mass distributions of surface waters on the Belizean shelf (BS). The newly developed two-way nesting technique based on the smoothed semi-prognostic method (Sheng *et al.*, 2005 a)① was used to exchange information between sub-components of the nested model system and specify the open boundary conditions of the middle and inner models. The main advantage of the newly developed nesting technique is that it prevents unrealistic drift of the middle and inner models by adjusting large-scale circulations produced by the two models using the outer and middle model results, respectively, while the model temperature and salinity of the nested system are fully prognostic.

The triply nested-grid modeling system simulates reasonably well the general circulation in the upper ocean of the WCS. The monthly mean near-surface circulation in the BS produced by the fine-resolution inner model is characterized by a strong and persistent northwestward flow over the seaward areas of Lighthouse Reef Atoll (LRA) and Turneffe Island Atoll (TIA), apparently as a direct result of the interaction between the strong, directional Caribbean Current and the weak, spatially variable currents in the southern and inner BS. The monthly mean circulation produced

① Sheng, J., X. Zhai, and R. J. Greatbatch, 2005 a. Numerical study of the storm-induced circulation on the Scotian Shelf during Hurricane Juan using a nested-grid ocean model. *Prog. in Oceanogr.*, (in press).

by the nested system also has significant month-to-month variability, with relatively weaker near-surface currents in the shallow waters off LRA and TIA in February and November and stronger ones in May and August. These patterns reflect the variation in the surface wind stress.

The triply nested-grid system was also used to simulate the upper ocean circulation during Hurricane Mitch in late October and early November 1998. A brief discussion of the model results was provided in Section 4, and a detailed discussion of the model results will be presented elsewhere.

Acknowledgements

We wish to thank Bruce Hatcher, Peter Sale, Richard Greatbatch, Chris Mooers, Leo Oey, Jiuxing Xing and Xiaoming Zhai for their useful suggestions and comments. We thank David Fratantoni for his providing the near-surface currents determined from the 15 m-drogued satellite-tracked drifters in the North Atlantic, and Carsten Eden for his providing monthly-mean transports in the North Atlantic produced by FLAME. This study was supported by NASA (NNG04GO90G) to USF (subcontract: #2500-1083-00-A). JS is also supported by the NSERC/MARTEC/MSC Industrial Research Chair.

Appendix: The Two-Way Nesting Technique Based on the Smoothed Semi-Prognostic Method

The smoothed semi-prognostic (SSP) method (Eden *et al.*, 2004) is a modification of the original semi-prognostic (OSP) method introduced by Sheng *et al*. (2001). The original application of both SSP and OSP methods was to adjust an ocean circulation model to correct for systematic error by adding a correction term to the model hydrostatic equation. This technique is equivalent to adding a pressure-correction term to the horizontal momentum equation (Greatbatch *et al.*, 2004). The newly developed nesting technique based on the SSP method is equivalent to adding an interaction term to the model momentum equation in each sub-component of the nested system.

The SSP nesting technique has two major components (Sheng *et al.*, 2005 b①; Sheng and Tang, 2004; Tang *et al.*, 2005②): (i) the specification of the model open boundary conditions described in Section 2, and (ii) the use of the SSP method to exchange information between subcomponents of the nested-grid modeling system. The second component has three steps described as follows. First, the middle model temperature and salinity (TS) are interpolated onto the inner model grid to adjust the momentum equation of the inner model over the common sub-region where the inner and middle model grids overlap based on

$$\frac{\partial p_{\text{inn}}}{\partial z} = -g\rho_{\text{inn}} - g(1-\beta_{\text{inn}})<\hat{\rho}_{\text{mid}} - \rho_{\text{inn}}>, \qquad \text{(A1)}$$

where p_{inn} and ρ_{inn} are the pressure and density variables of the inner model, respectively, $\hat{\rho}_{\text{mid}}$ is density calculated from the middle model TS fields after interpolation onto the inner model grid, β_{inn} is the linear combination coefficient with a value between 0 and 1, and $<>$ is a filtering operator. The filtering operator ensures that the inner model is constrained by the middle model only on large scales (determined by the smoothing scale that is used), the smaller scales associated with the fine grid of the inner model being free to evolve without constraint.

Second, the middle model TS fields are interpolated onto the outer model grid to adjust the momentum equations of the outer model over the common sub-region where the outer and middle model grids overlap, based on

$$\frac{\partial p_{\text{out}}}{\partial z} = -g\rho_{\text{out}} - g(1-\beta_{\text{out}})<\tilde{\rho}_{\text{mid}} - \rho_{\text{out}}>, \qquad \text{(A2)}$$

where p_{out} and ρ_{out} are respectively the pressure and density variables of the outer model, $\tilde{\rho}_{\text{mid}}$ is density calculated from middle model TS fields after interpolation onto the outer model grid, β_{out} is the linear combination coefficient with a value between 0 and 1, and $<>$ is the filtering operator, which usually differs from that in Eq. (A1).

Third, the outer and inner model TS fields are interpolated onto the middle model grid to adjust the momentum equation of the middle model over the overlapping sub-region, based on

$$\frac{\partial p_{\text{mid}}}{\partial z} = -g\rho_{\text{mid}} - g(1-\beta_{\text{mid}})<\rho_{\text{opi}} - \rho_{\text{mid}}>, \qquad \text{(A3)}$$

where p_{mid} and ρ_{mid} are the pressure and density variables of the middle model respectively, $\tilde{\rho}_{\text{opi}}$ is density calculated from the outer and inner model TS fields after interpolation onto the middle model grid, and β_{mid} is the linear combination coefficient with a value between 0 and 1.

As discussed in Sheng *et al*. (2005 b)③, the above SSP nesting technique is equivalent to adding an interaction term to the model momentum equation in each sub-component of the nested system. The interaction term depends on the density difference between subcomponents of the nested system shown in the second terms in Eqs. (A1 - A3), with linear coefficients β_{inn}, β_{out} and β_{mid} determining the intensity of the interaction. In this study, we follow Sheng *et al.* (2005 b)④ and set the linear combination coefficients β_{inn}, β_{out} and β_{mid} to 0.5. Readers are referred to Sheng *et al*. (2005 b)⑤ for the choice of these coefficients. The filtering operator used in this study is the running averaging, with a smoothing scale of 24 km for the inner model, and 72 km for the middle model. The filtering operator in Eq. (A3) for the outer model is not used in this study. Since the model forcing is the monthly mean climatology in the first application discussed in Section 3, it is sufficient to exchange information between the subcomponents of the nested system once per day. In the second application of the nested-grid system discussed in Section 4, the exchange rate of the nested system is 10 times per day.

---

① Sheng, J., R. J. Greatbatch, X. Zhai, and L. Tang, 2005 b. A new two-way nesting technique based on the smoothed semi-prognostic method. *Ocean Dyn.*, (in press).

② Tang, L., J. Sheng, B. Hatcher, and P. Sale, 2005. Numerical study of circulation, dispersion and hydrodynamic connectivity of surface waters on the Belize shelf. *J. Geophs. Res.*, (in press).

③ Same as ①.

④ Same as ①.

⑤ Same as ①.

References

Andrade, C. A., and E. D. Barton, 2000. Eddy development and motion in the Caribbean Sea. *J. Geophys. Res.*, **105**: 26 191–26 201.

Barnier, B., L. Siefridt, and P. Marchesiello, 1995. Thermal forcing for a global ocean circulation model using a three year climatology of ECMWF analysis. *J. Mar. syst.*, **6**: 363–380.

Cesar, H. S. J., 2000. Their functions, threats and economic value. In: *Collected Essays on the Economics of Coral Reefs*, Coral Reefs. Cesar, H. S. J., ed., CORDIO, Sweden, 244 pp.

Chang, S. W., and R. A. Anthes, 1978. Numerical simulations of the ocean's nonlinear baroclinic response to translating hurricanes. *J. Phys. Oceanogr.* **8**: 468–480.

da Silva, A. M., C. C. Young, and S. Levitus, 1994. Anomalies of heat and momentum fluxes. In: *Atlas of Surface Marine Data*, Vol. 3. NOAA Atlas NESDIS 8, NOAA, Washington, D.C., 413 pp.

de Groot, R., M. Wilson, and R. Boumans, 2002. A typology for the classification, description and valuation of ecosystem functions, goods and services. *Ecol. Econ.*, **41**: 393–408.

Dengg, J., C. Boening, U. Ernst, R. Redler, and A. Beckmann, 1999. Effects of an improved model representation of overflow water on the subpolar North Atlantic. *International WOCE Newsletter*, **37**: 10–15.

Dietrich, D. E., 1997. Application of a modified Arakawa 'a' grid ocean model having reduced numerical dispersion to the Gulf of Mexico circulation. *Dyn. Atmos. and Oceans*, **27**: 201–217.

Eden, C., R. J. Greatbatch, and C. W. Boning, 2004. Adiabatically correcting an eddy-permitting model of the North Atlantic using large-scale hydrographic data. *J. Phys. Oceanogr.*, **34**: 701–719.

Ezer, T., L-Y Oey, and H-C Lee, 2003. The variability of currents in the Yucatan Channel: Analysis of results from a numerical model. *J. Geophys. Res.*, **108**: 3012, doi: 10.1029/2002JC001509.

Fratantoni, D. F., 2001. North Atlantic surface circulation during the 1990's observed with satellite-tracked drifters. *J. Geophys. Res.*, **106**: 22 067–22 093.

Gallegos, A., 1996. Descriptive physical oceanography of the Caribbean Sea. In: *Coastal and Estuarine Studies*, 51. *Small Islands: Marine Science and Sustainable Development*. Maul, G. A., ed., American Geophysical Union, Washington, D.C., 36–55.

Gibson, J., M. McField, and S. Well, 1998. Coral reef management in Belize: an approach through integrated coastal zone management. *Ocean and Coastal Management*, **39**: 229–244.

Gordon, A. L., 1967. Circulation of the Caribbean Sea. *J. Geophys. Res.*, **72**: 6 207–6 223.

Greatbatch, R. J., J. Sheng, C. Eden, L. Tang, X. Zhai, *et al.*, 2004. The semi-prognostic method. *Continental Shelf Res.*, **24**: 2 149–2 165.

Haney, R. L., 1971. Surface thermal boundary conditions for ocean circulation models. *J. Phys. Oceanogr.*, **1**: 241–248.

Hubbell, S. P., 1997. A unifield theory of biogeography and relative species abundance and its application to tropical rain forests and coral reefs. *Coral Reefs*, **16**: S9–S21.

Hurlburt, H. E., and T. L. Townsend, 1994. NRL effort in the North Atlantic. In: *Data Assimilation and Model Evaluation Experiments: North Atlantic Basin Preliminary Experiment Plan*. Willems, R. C., ed., Tech. Rep. TR-2/95, University of Southern Mississippi, Hattiesburg, Miss., 30–35.

Johns, W. E., T. L. Townsend, D. M. Fratantoni, and W. D. Wilson, 2002. On the Atlantic inflow to the Caribbean Sea. *Deep-Sea Res.*, **49**A: 211–243.

Kinder, T. H., G. W. Huburn, and A. W. Green, 1985. Some aspects of the Caribbean circulation. *Marine Geology*, **68**: 25–52.

Large, W. G., J. C. McWilliams, and S. C. Doney, 1994. Oceanic vertical mixing: A review and a model with a nonlocal boundary layer parameterization. *Rev. Geophys.*, **32**: 363–403.

Macintyre, I. G., and R. B. Aronson, 1997. Field guidebook to the reefs of Belize. *Proc. 8th Int. Coral Reef Symp.*, 203–221.

Marchesiello, P., J. C. McWilliams, and A. Shchepetkin, 2001. Open boundary conditions for long-term integration of regional oceanic models. *Ocean Model.* **3**: 1–20.

Maul, G. A., 1993. *Climatic Change in the Intra-Americas Sea*. United Nations Environment Programme, Edward Arnold, London, 389 pp.

Mooers, C. N. K., and G. A. Maul, 1998. Intra-Americas Sea Circulation, Coastal Segment (3, W). In: *The Sea*, 11. John Wiley and Sons, 183–208.

Murphy, S. J., H. E. Hurlburt, and J. J. O'Brien, 1999. The connectivity of eddy variability in the Caribbean Sea, the Gulf of Mexico, and the Atlantic Ocean. *J. Geophys. Res.*, **104**: 1 431–1 453.

Nystuen, J. A., and C. A. Andrade, 1993. Tracking mesoscale ocean features in the Caribbean Sea using Geosat Altimetry. *J. Geophys. Res.*, **98**: 8 389–8 394.

Orlanski, I., 1976. A simple boundary condition for unbounded hyperbolic flows. *J. Comput. Phys.*, **21**: 251–269.

Roemmich, D., 1981. Circulation of the Caribbean Sea: a well-resolved inversed problem. *J. Geophys. Res.*, **86**: 7 993–8 005.

Sheng, J., and L. Tang, 2003. A numerical study of circulation in the western Caribbean Sea. *J. Phys. Oceanogr.*, **33**: 2 049–2 069.

Sheng, J., and L. Tang, 2004. A two-way nested-grid ocean-circulation model for the Meso-American Barrier Reef System. *Ocean Dyn.*, **54**: 232–242.

Sheng, J., and L. Wang, 2004. Numerical study of tidal circulation and nonlinear dynamics in Lunenburg Bay, Nova Scotia. *J. Geophys. Res.*, **109**: C10018, doi: 10.1029/2004JC002404.

Sheng, J., D. G. Wright, R. J. Greatbatch, and D. E. Dietrich, 1998. CANDIE: A new version of the DieCAST ocean circulation model. *J. Atmos. and Ocean. Tech.*, **15**: 1 414–1 432.

Smagorinsky, J., 1963. General circulation experiments with the primitive equation. I. The basic experiment. *Mon. Wea. Rev.*, **21**: 99–165.

Thuburn, J., 1996. Multidimensional flux-limited advection schemes. *J. Comput. Phys.*, **123**: 74–83.

Williams, E. H., and L. Bunkley-Williams, 2000. Marine major ecological disturbances of the Caribbean. *Infec. Dis. Rev.*, **2**: 110–127.

Wust, G., 1964. *Stratification and Circulation in the Antillean-Caribbean Basins, Part One, Spreading and Mixing of the Water Types with an Oceanographic Atlas*. Columbia University Press, New York, 201 pp.